Photophysics and X-ray structure of crystalline 2-aminopurine

Manuscript received: 19/09/2006; Revised: 26/02/2007; Article published: 27/03/2007

Photophysics and x-ray structure of crystalline 2-aminopurine**

Dr. Robert K. Neely,[1,2] Dr Steven W. Magennis,[1,2] Dr Simon Parsons[1] and Dr Anita C. Jones[1,2,*]

[1]EaStCHEM, School of Chemistry, Joseph Black Building, University of Edinburgh, West Mains Road, Edinburgh, EH9 3JJ, UK.

[2]Collaborative Optical Spectroscopy, Micromanipulation and Imaging Centre (COSMIC), The University of Edinburgh, West Mains Road, Edinburgh, EH9 3JZ, UK.

[*]Corresponding author; e-mail: a.c.jones@ed.ac.uk, fax: +44(0)131 6506453

[**]We are grateful to Dr David Dryden for helpful discussions and to the Engineering and Physical Sciences Research Council and the Scottish Higher Education Funding Council for financial support.

Supporting information:
Supporting information for this article is available on the WWW under http://www.wiley-vch.de/contents/jc_2267/2007/f600593_s.html, or from the author.

Graphical abstract:

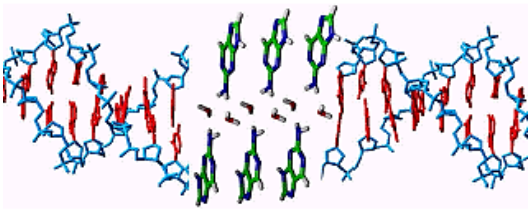

Synopsis:
Interbase interactions in DNA are mimicked in the crystal lattice of 2-aminopurine, a fluorescent analogue of adenine. π-stacking interaction between 2-aminopurine moleules in the crystal produces a low energy excited state, showing red-shifted emission.

Keywords:
DNA; fluorescence; fluorescence lifetime; nucleic acids; X-ray diffraction

Abstract

To explore the effect of intermolecular interactions on the photophysics of 2-aminopurine (2AP) in a well-defined environment, we have investigated the fluorescence properties of single 2AP crystals, having determined the x-ray structure. In the crystal, 2AP is subject to base-stacking and hydrogen-bonding interactions similar to those found in DNA. The crystal shows dual fluorescence: π-stacked molecules in the bulk of the lattice have red-shifted excitation and emission spectra, while molecules at defect sites have spectra similar to those of 2AP in solution or in DNA. Heterogeneous intermolecular interactions in the crystal give rise to multiexponential fluorescence decay characteristics similar to those observed for 2AP-labelled DNA. The presence of about 13% of the 7H tautomer in the crystal confirms that 9H-7H tautomerisation of 2AP occurs in the ground state. Long-wavelength excitation of a 2AP-labelled oligonucleotide duplex produced red-shifted emission similar to that observed in the crystal, indicating that π-stacking interaction of 2AP with nucleobases gives rise to a low energy excited state.

Introduction

Fluorescence spectroscopy has a central role to play in advancing understanding of DNA dynamics and the mechanisms by which DNA interacts with proteins and other ligands. The application of fluorescence techniques to nucleic acids requires the insertion of a suitable fluorophore into the helix, because the natural bases have very low fluorescence quantum yields.[1] 2-aminopurine (2AP), a structural analogue of adenine, is widely used as a *quasi*-intrinsic fluorescent probe of the structure and dynamics of DNA[2-10] and their influence on electron transport in the helix. [11-17] 2AP forms Watson-Crick base pairs with thymine and, therefore, does not disrupt the DNA double helical structure.[18] Furthermore, the absorption maximum of 2AP (305 nm) is red-shifted relative to the natural bases, allowing selective excitation[19], and its fluorescence properties are sensitive to the local molecular environment.[20;21]

In aqueous solution 2AP riboside shows a single fluorescence lifetime of 10.6ns.[22] In contrast, the fluorescence decay of 2AP in DNA is highly non-exponential; typically it can be described by the sum of four exponential components[8;23-26] with lifetimes of <100ps, ~0.5ns, ~2ns and ~10ns. This complex decay behaviour is generally accepted to reflect a multiplicity of conformational states in which 2AP experiences different intermolecular interactions, including varying degrees of stacking. At present, interpretation of the response of 2AP fluorescence to the local environment within the DNA helix is hampered by an incomplete understanding of the photophysical effects of interbase interactions.

To explore the photophysics of 2AP in a well-defined, static molecular environment we have grown single crystals of 2AP, determined their crystal structure and investigated their fluorescence properties. We find analogies between both the interbase interactions and photophysical properties of crystalline 2AP and those of

2AP in the DNA duplex. To our knowledge, there have been no previous structural or spectroscopic studies of 2AP in the crystalline phase, although the crystal structures of three C6-substituted 2AP derivatives[27] and of 9-[4-acetoxy-3-(acetoxymethyl)-butyl]-2-aminopurine[28] have been reported.

In a study of the polarised reflectance spectra of single crystalline adenine, Chen and Clark found evidence of exciton coupling between adenine molecules, manifested as Davydov splitting[29]. A solution phase study by Rist *et al*[30] of a DNA duplex containing four pairs of adjacent 2AP bases, revealed a new weak emission band, red-shifted with respect to the typical 2AP fluorescence spectrum, and a corresponding red-shifted excitation spectrum. This indicated a significant ground-state interaction between adjacent 2AP bases, to form a dimer-like state in which the excitation is delocalised over the coupled monomers. Evidence for weak exciton coupling between 2AP and other bases was also presented. The excitonic interaction between adjacent 2AP bases in DNA has also been used a mechanism for studying the conformational dynamics of DNA by circular dichroism spectroscopy.[31] We show here that interaction between 2AP molecules in the π-stacked structure of the crystal lattice produces a low energy excited state, giving rise to red-shifted fluorescence with an emission maximum of ~ 420 nm and an excitation maximum of ~370 nm.

Results and Discussion

Crystal Structure: The asymmetric unit of the 2AP crystal consists of one molecule of monohydrated 2AP, the structure of which is shown in Figure 1(a). The 2AP molecule is planar apart from the protons of the amine group which lie slightly out of plane. There is a strong hydrogen bond (N···H=1.974 Å) between the water (H11) and N7 of 2AP. Electron density peaks in the Fourier difference map indicate disorder in the crystal structure corresponding to a hydrogen atom (H7) bound to N7, with an occupancy of 0.13(3) Thus, 13% of the 2AP molecules in the crystal exist as the 7H tautomer. This is consistent with our findings from fluorescence lifetime measurements on 2AP in solution, which showed about 20% of the 7H tautomer to be present in ethanol solution.[22] and confirms that 9H-7H tautomerisation occurs in the ground state, in agreement with the recent theoretical study by He *et al.*[32] In conjunction with the 7H tautomer, the water molecule adopts a different orientation, with its protons in sites H13 and H14, as shown in Figure 1(a), and its oxygen hydrogen-bonded to H7 of 2AP.

The bond lengths and bond angles derived from the crystal structure are shown in Table 1. Selected bond lengths are shown in Figure 1(b) together with those calculated for the 9H 2AP tautomer[33] and those measured by x-ray crystallography for 2-amino-6-chloropurine.[27] In general, there is good agreement between the two x-ray structures. Comparison with the structure calculations of Broo[33] for 2AP shows that the measured N9-C8 bond length is shorter than that predicted for the 9H tautomer, and the N7-C8 bond length longer. This is consistent with the presence in the crystal of 13% of the 7H tautomer which has a substantially shorter N9-C8 bond and longer N7-C8.[33]

Bond Lengths (Å)		Bond Angles (deg)	
N1-C2	1.365(2)	N1-C2-N3	126.54(19)
N1-C6	1.332(3)	N1-C2-N21	116.11(18)
C2-N3	1.343(2)	N1-C2-N21	117.34(17)
C2-N21	1.353(3)	C2-N3-C4	112.42(16)
N3-C4	1.329(3)	N3-C4-C5	126.52(18)
C4-N9	1.368(3)	C4-C5-C6	115.85(18)
C4-C5	1.400(2)	C5-C6-N1	120.33(17)
N9-C8	1.360(3)	C6-N1-C2	118.33(17)
N9-H9	0.871(9)	N3-C4-N9	127.82(17)
C8-N7	1.318(2)	C4-C5-N7	110.04(16)
C8-H8	0.97(2)	C5-N7-C8	103.93(17)
N7-C5	1.389(3)	N7-C8-N9	113.91(19)
C5-C6	1.381(3)	N8-N9-C4	106.45(16)
C6-H6	0.95(2)		
N21-H211	0.890(9)		
N21-H212	0.883(9)		

Table 1. Bond lengths and bond angles of 2AP.H_2O

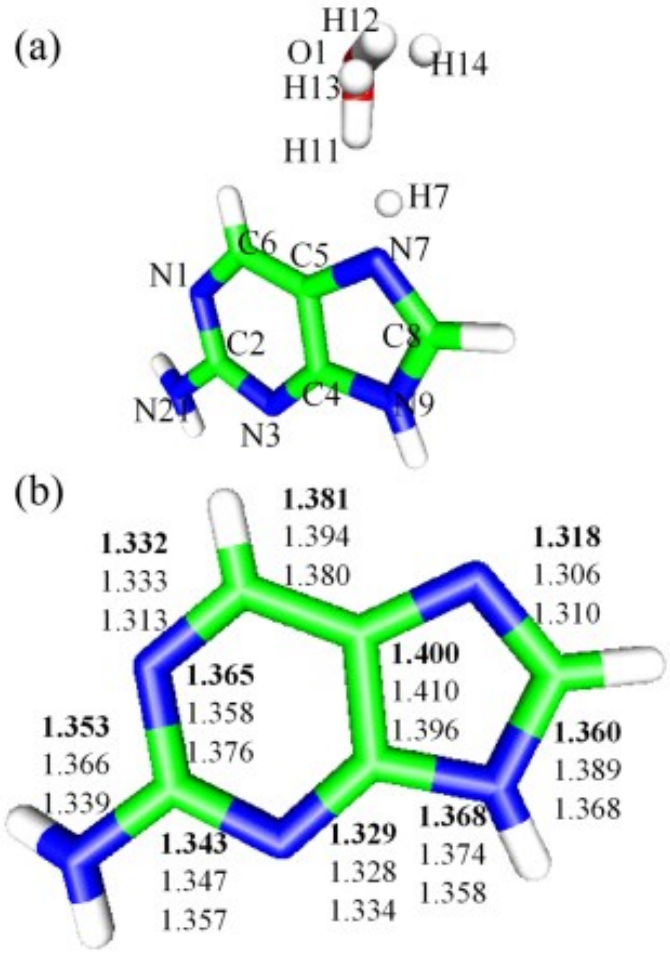

← ***Figure 1.*** (a) The asymmetric unit and numbering scheme for 2AP.H_2O in the crystal structure. (b) The bond lengths (Å) determined in the present work (top, bold); those calculated for the 9-H tautomer of 2AP[33] (middle); those for the x-ray structure of 2-amino-6-chloropurine[27] (bottom).

Figure 2 shows the unit cell which contains four 2AP.H_2O molecules. An extensive hydrogen bonding network is apparent. As shown in Figure 3(a), adjacent 2AP molecules hydrogen bond through an N9H to N1 interaction, and each 2AP molecule is hydrogen bonded to 3 neighbouring water molecules via N7 and the two amine protons. The hydrogen bonds formed in the crystal are all of moderate strength with those involving ring atoms being around 0.2Å shorter than those of the amine group.

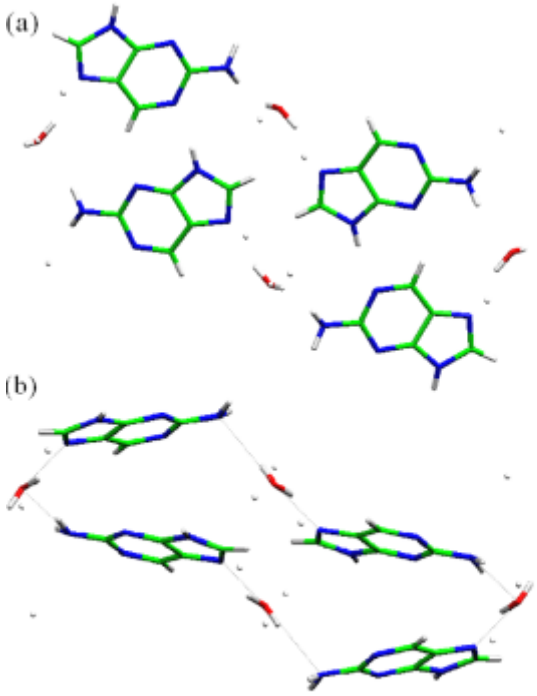

Figure 2. (a) The unit cell of the 2AP.H_2O crystal viewed along the crystallographic a-axis. (b) Illustration of the packing of molecules in the unit cell.

The hydrogen bonding interactions of 2AP in the crystal mimic those that the molecule experiences in the DNA duplex, where 2AP base-pairs with adenine, thymine or cytosine via hydrogen bonding at one of the amino protons and at N1. In the DNA duplex, ordered solvation shells of water are formed in both the minor and major grooves.[34] In this water-rich environment, the free amine proton and N7 of 2AP are likely to be hydrogen-bonded to water molecules, as in they are in the crystal.

Extended columns of π-stacked 2AP molecules are present in the crystal, as illustrated in Figure 3(b). The closest contacts between adjacent molecules in these stacks are between C5 and C6 (3.256Å) and between C8

and C5 (3.338Å). Thus, molecules in the stack are staggered, with the imidazole and pyrimidine rings of adjacent molecules overlapping. The centre of the imidazole ring of each molecule lies above the C8 atom of the molecule below it in the stack. In many ways, the interaction between 2AP molecules in these stacks mimics base-stacking interactions in the DNA duplex. Hassan and Calladine have reviewed the structures of some 60 DNA duplexes[35] and show that the rise between adjacent base steps is essentially sequence independent and has a magnitude of 3.4Å. Adjacent DNA bases are also offset relative to one another, as are the 2AP molecules in the crystal, though this 'slide' parameter varies in a sequence specific manner. The 2AP crystal does not, however, mimic the rotational displacement (twist) of the DNA bases. In the crystal, there is no rotational displacement between adjacent molecules in the π-stack, whereas in DNA there is a rotational offset of ~36 ^{o} between adjacent bases.

Steady-State Fluorescence Spectra: Single-crystal 2AP shows two distinct emission bands, each with its own excitation spectrum, indicating the presence of two ground state species with quite different electronic structures. As shown in Figure 4, excitation of the crystal at 300nm or less gives an emission spectrum that resembles that of 2AP in aqueous solution, with a peak at around 370nm. Excitation at longer wavelength results in red-shifted emission peaking at around 420nm. The excitation spectra of the two emission bands are shown in Figure 5. The short-wavelength emission band (Figure 4) is somewhat broadened to longer wavelength compared with the spectrum of 2AP in solution because of a contribution from the long-wavelength band that is also excited at 300nm, as shown in Figure 5. Similarly, the peak of the excitation spectrum of the short wavelength emission appears red-shifted relative to that of 2AP in solution (Figure 5) because long wavelength emission is also being detected at 360 nm. The overlap between the spectra of the two species prevents a quantitative measurement of their relative emission intensities: although the long wavelength emission band can be excited selectively, the short wavelength band always contains a contribution from the more intense long wavelength emission. However, we estimate that the longer wavelength emission is approximately five times more intense than the short wavelength emission, at their respective excitation maxima (370 nm and 300 nm).

On dissolution of crystalline 2AP in water, the long wavelength emission is lost and only the short wavelength emission characteristic of free 2AP (Figure 4) remains. The long wavelength excitation and emission spectra must result from interactions between 2AP molecules in the crystal, that is, the hydrogen bonding and π-stacking interactions shown in Figure 3(b). Very similar spectra were reported by Rist et al[30] for a 2AP-labelled DNA duplex containing pairs of adjacent 2AP base, showing that. interaction between the adjacent 2AP bases gives rise to a dimer-like species with lower excitation energy than free 2AP. This suggests that in the crystal the major influence on the excitation energy of 2AP is the interaction between adjacent molecules in the π stack. The predominant long wavelength emission of the 2AP crystal can thus be attributed to dimer- or trimer-like species resulting from ground-state interaction between neighbouring molecules in the π stack, as illustrated in Figure 6. Hereafter we will call the long-wavelength emitting species "stacked 2AP".

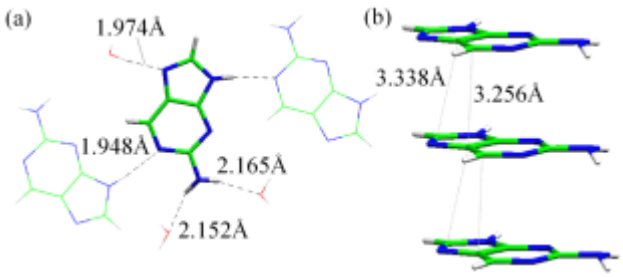

Figure 3. Intermolecular interactions in the 2AP crystal. (a) Hydrogen bonds (proton to acceptor distances are shown); (b) π-stacking interactions.

The short wavelength excitation and emission spectra are characteristic of 2AP molecules that are not perturbed by intermolecular interactions. In the crystal, such species can be found at defect sites where the lattice is locally disordered and molecules are translated, twisted or tilted relative to their neighbours in the π-stack, as illustrated in Figure 6. Whilst all molecular crystals contain defects[36] due to structural flaws or impurities, in the present case an obvious source of lattice imperfections is the presence of a small fraction of the 7H tautomer. The 7H tautomer differs from the 9H tautomer in both its dipole moment (magnitude and direction)[33] and hydrogen bonding sites, and its presence will cause local disruption of intermolecular interactions. The short wavelength emission may arise from the 7H tautomer itself or from 9H molecules in the locally disrupted lattice. 2AP molecules at surface sites may also show emission characteristic of the free molecule. The short-wavelength emitting species will be referred to hereafter as "unperturbed 2AP".

The spectral perturbation induced by intermolecular interaction in a crystal has two contributions: (i) the difference in the intermolecular interaction energy (e.g. dipole-dipole, dipole-induced dipole, dispersion etc.) of the molecule with its neighbours in its ground state and in its excited state; (ii) the resonance interaction energy or exciton coupling[37]. A mean shift of the excitation energy (relative to the free molecule) is caused as a result of (i) and the exciton coupling between translationally *equivalent* molecules in the lattice. Exciton coupling between tranlationally *inequivalent* molecules causes splitting (Davydov splitting) of the molecular excited state into a number of exciton states, some of which may be forbidden or only weakly allowed. The presence of four 2AP molecules in the unit cell should give rise to four exciton states for each free molecule state. Emission will occur from only the lowest exciton state (in accordance with Kasha's rule), but higher lying, allowed states should be apparent in the excitation spectrum. The excitation spectrum of stacked 2AP (Figure 5) shows no obvious sign of splitting. The band maximum at ~370nm corresponds to direct excitation into the emitting state (the Stokes shift is comparable to that between the excitation and emission maxima of the unperturbed molecule). However, there is a weak short wavelength tail on the excitation spectrum that extends to about 270nm, overlapping with the unperturbed 2AP spectrum. Comparison of the crystal emission spectrum excited at 280nm with that of 2AP in solution (Figure 5) confirms that excitation in this short wavelength region results in a significant intensity of red-shifted, stacked AP emission. This may be indicative

of excitation via higher energy crystal states, but could also be due to excitonic energy transfer from unperturbed 2AP to stacked 2AP. The failure to positively identify Davydov splitting could be because the splittings are unresolvable, given the broadness of the excitation spectrum, and/or the transitions to higher exciton states are of low intensity.

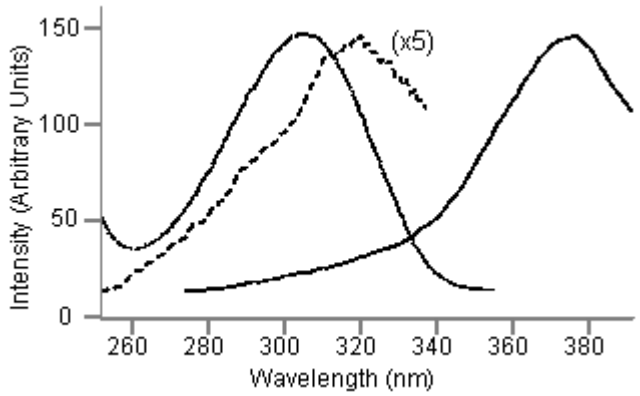

Figure 5. Excitation spectra of 2AP crystal at emission wavelengths of 360 nm (dashed line; intensity multiplied by a factor of 5) and 440 nm (solid line). Also shown for comparison is the excitation spectrum for 2AP in water at an emission wavelength of 370 nm (dotted line).

The shift in excitation energy due to excitonic interaction between two neighbouring molecules in the same π stack (translationally equivalent molecules) can be estimated using the point-dipole model[38] , in which the interaction between the transition densities is approximated by the dipole-dipole energy, Λ:

$$\Lambda = \frac{1}{4\pi\varepsilon_0}\frac{\mathbf{M}_1\mathbf{M}_2}{R^3} - \left(\frac{3(\mathbf{M}_1 \bullet \mathbf{R})(\mathbf{M}_2 \bullet \mathbf{R})}{R^5}\right) \qquad (1)$$

where $\mathbf{M}_1$ and $\mathbf{M}_2$ are the transition dipole moments (in Cm), **R** is the vector separation of the transition dipole centres (in m) and ε_0 is the permittivity of free space. For identical molecules ($\mathbf{M}_1 = \mathbf{M}_2$**),** lying in parallel planes, this becomes :

$$\Lambda = \frac{1}{4\pi\varepsilon_0}\frac{|\mathbf{M}|^2}{R^3}\left(1 - 3\cos^2\theta\right) \qquad (2)$$

where θ is the angle between **R** and the transition moment. The S_0-S_1 transition of 2AP is nominally long-axis polarised, but experiment[39] and theory[40,41] indicate that the transition moment is rotated ~30° clockwise from the long axis. The transition moment is related to the oscillator strength f:

$$f = 4.227 \times 10^{52} \bar{\nu} |\mathbf{M}|^2 \qquad (3)$$

where $\bar{\nu}$ is the wavenumber of the electronic transition (in cm^{-1}). Thus the exciton interaction energy (in J) is given by:

$$\Lambda = \frac{f}{4.703 \times 10^{42} \bar{\nu} \, R^3} \left(1 - 3\cos^2 \theta\right) \qquad (4)$$

From the crystal structure, R = 3.63 Å and θ = 77.5°. Taking $\bar{\nu}$ to be 32370 cm^{-1} [42] and f to be 0.10[39] gives a value of +590 cm^{-1} for Λ; this is an increase in excitation energy, since the dipole-dipole interaction is repulsive for 54.74° < θ ≤ 90°. Thus, the principal influence on the excitation energy of stacked 2AP appears to be an increase in the intermolecular interaction energy on excitation, resulting in the observed red shift of around 5000 cm^{-1} relative to the unperturbed molecule. The magnitude of this shift suggests considerable charge transfer (orbital overlap) between neighbouring molecules.

Time-Resolved Fluorescence: Fluorescence decay curves of the crystal species, unperturbed 2AP and stacked 2AP, were recorded at excitation wavelengths of 300nm and 400nm, respectively, and over a range of detection wavelengths across the two emission bands.

Unperturbed 2AP: Unperturbed 2AP showed a multiexponential decay that could be fitted globally by 4 common lifetimes across the emission envelope. The lifetimes and A factors are given in Table 2. Fits made using only three lifetimes gave significantly poorer results, with χ^2 values typically of 1.7- 1.8. The observation of a multiexponential decay indicates that the emitting unperturbed 2AP molecules exist in a heterogeneous environment, with the different decay components representing populations of 2AP molecules subject to different intermolecular interactions in the crystal lattice. This behaviour is as might be expected for molecules associated with lattice defects which are unlikely to be uniform in their local structure.

Emission wavelength [nm]	A_1	A_2	A_3	A_4	Local χ^2
350	0.73	0.22	0.05	0.00	1.13
360	0.76	0.17	0.06	0.01	1.04
370	0.75	0.18	0.06	0.01	1.09
390	0.72	0.20	0.07	0.01	1.06
410	0.72	0.20	0.07	0.01	1.08

Global lifetimes: τ_1=0.04ns, τ_2=0.30ns, τ_3=1.18ns, τ_4=4.85ns; Global χ^2 =1.07

Table 2. Fluorescence decay parameters for unperturbed 2AP in the single crystal. Fluorescence was excited at 300nm and decays obtained at the 6 emission wavelengths shown were fitted globally to 4 common lifetimes. The global fluorescence lifetimes and global χ^2 are given, followed by the A factors and local χ^2 for each decay.

Although four decay components were required to fit the decay data satisfactorily, the amplitudes of the two components with the longest lifetimes, 1.18 and 4.85ns, are very small; together these represent less than 10% of the emitting unperturbed 2AP molecules. (At the shorter emission wavelengths, these components are negligible). The dominant emitting species, >70% of the population, has a very short lifetime of 40ps. A second species with a lifetime of 300ps constitutes a significant fraction (>10%) of the emitting molecules.

The fluorescence spectrum typical of 2AP in DNA is very similar to that of unperturbed 2AP in the crystal (as shown below) and the characteristic 4-component decay of 2AP in DNA also resembles that observed here. Typical decay parameters for 2AP in a DNA duplex[26]are given in Table 3. In the duplex, as in the crystal, 70% of the emitting population has a very short decay time of 40ps. In DNA an efficient non-radiative decay channel is known to be electron transfer between excited 2AP and neighbouring bases, particularly guanine.[11-17,43] In this duplex, the 2AP is base is stacked between two guanines and is also paired with guanine. In the crystal there are apparently equally efficient non-radiative pathways. A significant non-radiative decay process for unperturbed 2AP in the crystal is likely to be energy transfer to the lower excitation energy species of the surrounding lattice (stacked 2AP).

τ_1/ns	τ_2/ns	τ_3/ns	τ_4/ns	A_1	A_2	A_3	A_4
0.04	0.50	2.9	11.0	0.70	0.12	0.10	0.08

Table 3. Fluorescence decay parameters of a 2AP-labelled DNA duplex (a 37-mer in which 2AP is paired with guanine and stacked between two guanines). Fluorescence was excited at 320 nm and detected at 390 nm.

Energy transfer, like electron transfer, is sensitive to the separation and relative orientation of the stacked bases. In both DNA and the crystal, the heterogeneous decay of 2AP arises from variation in interbase stacking interactions and the consequent variation in intermolecular quenching rate. A significant difference, in this respect, between the 2AP crystal and the DNA duplex is that the former is static whereas the latter is conformationally dynamic. Even in the geometrically constrained, crystalline environment, the variation in intermolecular interaction is sufficient to induce a variation of two orders of magnitude in the non-radiative decay rate, comparable to the range seen in DNA. Thus, although in DNA the decay of 2AP is influenced by base motion, such motion is not a pre-requisite for the observation of widely varying decay times. Recent studies [14, 44], in which duplex DNA was frozen in a rigid matrix at 77K, have elucidated the role of base dynamics in quenching of 2AP fluorescence. It has been shown that the highly stacked geometry that gives rise to the very short decay time of 2AP-labelled DNA is attained only through thermal motion of the bases[44] . In the 2AP crystal, however, the static geometric arrangement of molecules is pre-disposed to rapid intermolecular quenching. 2AP-containing dinucleotides, in which the interaction is limited to a single neighbouring base, also appear to show rapid quenching without base motion. In a recent study of dinucleotides of 2AP with guanine, adenine, thymine, cytosine and inosine, Somsen *et al*[45] attribute a very short exponential decay component (20-30 ps) to rapid quenching in the equilibrium stacked conformation, without base dynamics, whilst a much longer (~1 ns) stretched exponential component is associated with diffusive dynamics towards the equilibrium conformation.

Stacked 2AP: A naïve expectation would be that stacked 2AP, representative of the homogeneous, bulk crystal lattice, might show a simple fluorescence decay. However, this is not the case. As shown in Table 4, the decays are multiexponential and can be fitted by four global lifetimes over the emission range.

The results of Rist *et al* [30] show that perturbation of a 2AP molecule by stacking with one neighbour (i.e a dimeric interaction) is sufficient to produce a red-shifted emission spectrum very similar to that observed here for stacked 2AP in the crystal. The interaction of 2AP with a second neighbour in the crystal lattice (a trimeric interaction) appears to have little additional effect on the spectrum. Therefore, the heterogeneous decay of the long wavelength emission can be interpreted in terms of the presence of a number of stacked geometries in which 2AP is closely overlapped with one neighbour but has different degrees of overlap with its second neighbour in the stack, as illustrated in Figure 6. The lifetimes of these stacked species are substantially longer than those of the short-wavelength-emitting, unperturbed 2AP molecules. The predominant, shortest lifetime component of 120ps may be attributed to the perfectly stacked, trimer-like species, found in defect-free regions of the crystal lattice. In common with all molecular crystals, a major non-radiative decay channel will be excitonic energy transfer. Rapid exciton migration through the crystal lattice occurs, until a defect with lower excitation energy (a trap) is encountered, resulting in irreversible energy transfer. Examination of the dependence of the A factors on emission wavelength (Table 4) suggests that the longer-lived species have lower excitation energies than the short-lived species, which is consistent with energy transfer being an important decay mechanism.

Emission wavelength / nm	A_1	A_2	A_3	A_4	Local χ^2
430	0.60	0.29	0.10	0.01	1.12
460	0.56	0.28	0.14	0.02	1.07
490	0.41	0.36	0.21	0.03	1.07
520	0.39	0.34	0.24	0.03	1.08

Global lifetimes: τ_1=0.12ns, τ_2=0.56ns, τ_3=1.56ns, τ_4=6.13ns; Global χ^2=1.09

Table 4. Fluorescence decay parameters for stacked 2AP in the single crystal. Fluorescence was excited at 400 nm and decays obtained at the 4 emission wavelengths shown were fitted globally to 4 common lifetimes. The global fluorescence lifetimes and global χ2 are given, followed by the A factors and local χ^2 for each decay.

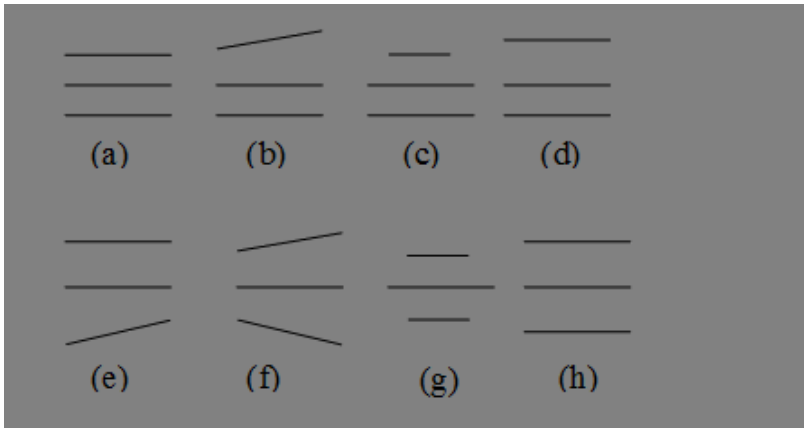

Figure 6. Schematic illustration of stacking arrangements that could result in long wavelength emission, (a) to (d), and short wavelength emission, (e) to (h). In conformations (a) to (d), corresponding to stacked 2AP, at least two of the bases are in a closely stacked, eclipsed arrangement. In conformations (e) to (h) corresponding to unperturbed 2AP, interaction between neighbouring bases is weakened by relative translation, tilting or twisting.

2AP in DNA: In studies of 2AP-labelled DNA, typically an excitation wavelength of around 300nm is used and the observed emission is similar to that of free 2AP, peaking at about 370nm. Prompted by our observation of a low energy emissive state for π-stacked 2AP and the observation of similar emission by Rist et al[30] for oligonucleotides containing multiple 2AP bases, we have investigated duplexes containing a single 2AP to see if excitation at wavelengths longer than those normally used would reveal red-shifted emission. Results for the duplex discussed above, in which 2AP is paired and stacked with G, are shown in Figure 7. Excitation at 300nm produces a short-wavelength emission spectrum that closely resembles that observed for the 2AP crystal at short excitation wavelengths (Figure 4). The emission band peaks at about 370nm, but is broadened considerably to the red compared with the spectrum of the free molecule in aqueous solution.

Excitation at 360nm does indeed give rise to longer wavelength emission with a maximum at about 430nm. This emission is substantially weaker than the short wavelength band, having only about one quarter the intensity. We have observed similar red-shifted emission from a number of 2AP-labelled duplexes and a full account of this work will be reported in a future publication.

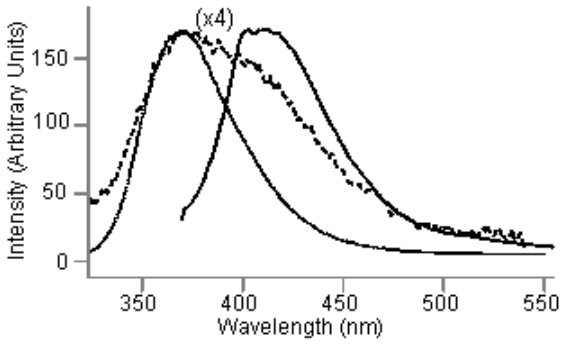

Figure 4. Emission spectra of 2AP crystal at excitation wavelengths of 280 nm (dashed line; intensity multiplied by a factor of 4) and 360 nm (solid line; contains a Raman band at 402 nm). Also shown for comparison is the emission spectrum of 2AP in water at an excitation wavelength of 300 nm (dotted line).

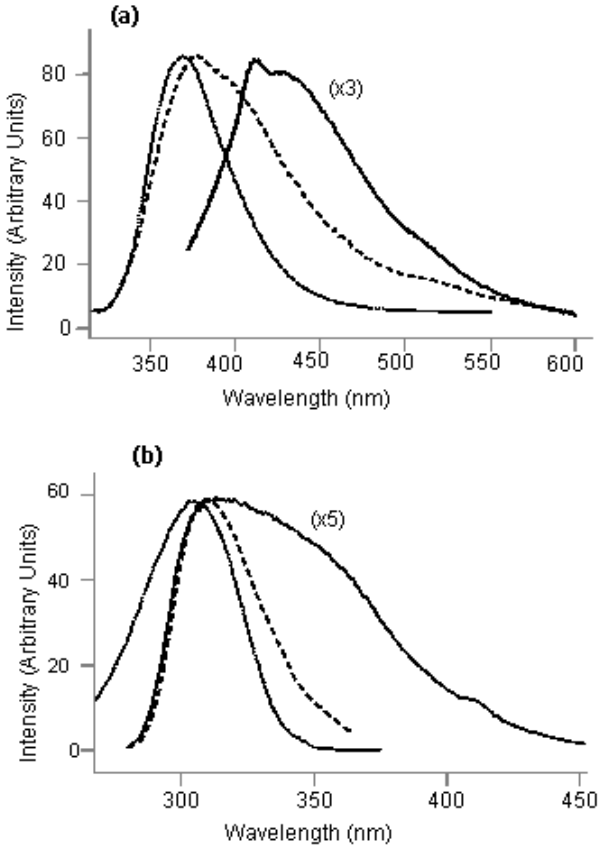

Figure 7. Emission and excitation spectra of a 2AP-labelled DNA duplex, in which 2AP is stacked between two guanines and paired with guanine. (a) Emission spectra at excitation wavelengths of 300 nm (dashed line)

and 360 nm (solid line; contains a Raman band at 410 nm). Also shown for comparison is the emission spectrum of 2AP in water at an excitation wavelength of 300nm (dotted line). (b) Excitation spectra at emission wavelengths of 380 nm (dashed line) and 480 nm. Also shown for comparison is the excitation spectrum of 2AP in water at an emission wavelength of 390 nm (dotted line).

In the duplex, the intensity of the red-shifted emission is low relative to the short wavelength band, whereas in the 2AP crystal the long wavelength emission of stacked 2AP is dominant. This may be due, to some extent, to differences in electronic structure between 2AP and the natural bases, but may also be related to a key difference in structure between the π-stack of duplex DNA and that of the 2AP crystal: there is a rotational offset (twist) of ~36 degrees between adjacent bases in the DNA helix which substantially reduces the π - overlap compared with the highly eclipsed stacks found in the crystal lattice. Indeeed, the predominant short-wavelength fluorescence of 2AP-labelled DNA resembles the emission of 2AP at defect sites in the crystal, where the molecules are displaced from the perfectly stacked structure. It seems likely that the long wavelength emission in DNA arises from particular conformational states of the duplex in which the rotational offset is reduced to give greater overlap between 2AP and its stacking partners. The low intensity of the emission suggests that these states constitute only a small fraction of the total population of base-stacked conformations of 2AP in the duplex.

Conclusions

The crystal structure of 2AP shows π-stacking and hydrogen-bonding interactions similar to those found in duplex DNA. Interaction between neighbouring 2AP molecules in the π-stacks results in fluorescence excitation and emission spectra that are substantially red-shifted relative to those of free 2AP. In addition to the predominant long-wavelength emission from stacked 2AP molecules in the bulk of the crystal lattice, there exist, at defect sites, 2AP molecules that are essentially unperturbed by intermolecular interactions and show short-wavelength excitation and emission spectra similar to those observed for 2AP in solution.

Although excitation of 2AP-labelled DNA duplexes at around 300 nm produces emission resembling that of unperturbed 2AP, excitation at longer wavelength gives rise to a low energy emission band, analogous to that seen for stacked 2AP in the crystal. Previously, low lying excited states have been predicted to exist in stacked 2AP-nucleobase dimers and trimers, but have been assumed to be dark states[46,47]. Our observations together with those of Rist *et al*[30] suggest that in 2AP-labelled duplexes, weak long wavelength emission coexists with the familiar intense, short-wavelength emission, but it may only be apparent at excitation wavelengths longer than those normally used to excite 2AP.

About 13% of 2AP molecules in the crystal exist as the 7H tautomer, confirming that 9H-7H tautomerisation occurs in the ground state, in agreement with previous solution-phase fluorescence measurements[22] and *ab initio* calculations.[32] The short-wavelength 2AP emission may be associated with the presence of the 7H tautomer in the lattice; it may originate from the 7H tautomer itself or from 9H molecules in the vicinity of a 7H tautomer, where the local lattice structure is disrupted.

In the geometrically constrained crystalline environment, 2AP shows similar non-exponential decay behaviour to that observed in the dynamic DNA helix. The sensitivity of the photophysics of 2AP to subtle variation in static intermolecular interactions is demonstrated by the observation that the heterogeneity of these interactions in the crystal lattice is sufficient to induce a variation of two orders of magnitude in the non-radiative decay rate. While conformational fluctuations undoubtedly influence the non-radiative decay of 2AP in DNA, such fluctuations are not a pre-requisite for the observation of heterogeneous fluorescence decay times.

Experimental Section

2-Aminopurine was purchased from Aldrich and used as received. Crystals were grown by slow evaporation from spectroscopic grade ethanol (Aldrich). Diffraction data were collected at 150 K on a Bruker Smart APEX diffractometer equipped with an Oxford Cryosystems low-temperature device. An absorption correction was applied using the multiscan procedure SADABS[48]. The structure was solved by direct methods (SIR92)[49], and refined by full-matrix least-squares against F^2 (CRYSTALS)[50]. All non-hydrogen atoms were refined with anisotropic displacement parameters, while H-atoms were located in difference Fourier syntheses. A weak difference synthesis peak next to N7 was interpreted as hydrogen-atom disorder, and weak peaks in the region of the water of crystallization appeared to confirm this. The part-weight hydrogen atoms attached to N7 and N9 were refined subject to the restraint that equivalent distances and angles involving the hydrogen atoms were similar. Explicit geometry restraints were applied to the water of crystallization. The occupancies of the two disorder components refined to 0.87 and 0.13(3). The final conventional R factor [based on F and 1133/1598 data with $F > 4\sigma(F)$] was 0.0507, and the final difference map extremes were + 0.22 and -0.23 eÅ^3. Full crystal data and refinement statistics are available in the Supporting Information for this article.

The DNA oligodeoxynucleotide (5'-ACTGGTACAGTATCAGGPGCTGACC CACAACATCCG-3'; 3'-TGACCATGTCATAGTCCGCGACTGGGTGTTGTAGG C-5', where P is 2AP) was gratefully received from the Klimasauskas group at the Institute of Biotechnology, Vilnius, Lithuania. The DNA duplex was annealed prior to use, where a 50% excess of the non-fluorescent strand was used to ensure that the all of the 2AP labelled oligodeoxynucleotide was in the duplex form. The final duplex concentration was 20μM.

Steady-state fluorescence measurements were made using a Jobin Yvon Spex Fluoromax spectrofluorimeter. Spectra of the crystal samples were recorded by delivering the excitation beam to the crystal through a fused silica optical fibre bundle. Emission was collected at approximately 45° to the excitation beam and conveyed to the spectrometer via a second optical fibre bundle.

Fluorescence lifetimes were determined by the time-correlated single photon counting method, using an Edinburgh Instruments spectrometer equipped with TCC900 photon counting electronics. Single crystals of 2AP were mounted in quartz capillaries (Hampton Research Corp) of 1mm diameter, which were in turn mounted on a translation stage within the spectrometer sample chamber. The excitation source was a tuneable, mode-locked Ti-Sapphire laser system (Coherent Mira Ti-Sapphire laser pumped by Coherent 10W Verdi), producing ~200fs pulses at a repetition rate of 76MHz. The pulse repetition rate was reduced to 4.75MHz using a pulse picker (Coherent 9200) and the light was frequency doubled or tripled using a Coherent 5-050 harmonic generator. Fluorescence emission was detected orthogonal to the excitation beam through a polariser set at the magic angle with respect to the vertically polarised excitation. A bandpass of 10nm was used in the emission monochromator and photons were detected using a cooled microchannel plate detector (Hammamatsu R3809 series). The instrument response function, measured by scattering the excitation beam from a dilute suspension of colloidal silica (ludox), was 50ps FWHM.

Fluorescence decay curves were recorded on a timescale of 20ns, resolved into 4096 channels, to a total of 10000 counts in the peak channel. Decay curves were analysed using a standard iterative reconvolution method in the F900 (Edinburgh Instruments Ltd) and FAST (Alango Ltd) software packages. A multiexponential decay function (Equation 1) was assumed.

$$I(t) = \sum_{i=1}^{n} A_i \exp\left(\frac{-t}{\tau_i}\right) \qquad (1)$$

where A_i is the fractional amplitude and τ_i is the fluorescence lifetime of the ith decay component.

The quality of fit was judged on the basis of the reduced chi-square statistic, χ^2, and the randomness of residuals. Typically, we find that a χ^2 value <1.2 indicates an acceptable fit. In global analysis, a family of decay curves was fitted simultaneously, with lifetimes, τ_i, as common parameters.

References

[1] P.R. Callis, *Ann Rev Phys Chem* **1983**, *34*, 329-357.

[2] L. Stryer, D.C. Ward, E. Reich, *J.Bio.Chem.* 1969, *244*, 1228-1237.

[3] T.J. Su, B.A. Connolly, C. Darlington, R. Mallin, D.T.F. Dryden, *Nucl.Acids.Res.* **2004**, *32*, 2223-2230.

[4] B. W. Allan, N.O. Reich, *Biochemistry* **1996**, *35*, 14757-14762.

[5] Y.V. R. Reddy, D.N. Rao, *J.Mol Biol* **2000**, *298*, 597-610.

[6] B. Holz, S. Klimasauskas, S. Serva, E. Weinhold, *Nucl.Acids.Res.* **1998**, *26*, 1076-1083.

[7] J.T. Stivers, *Nucl.Acids.Res.* **1998**, *26*, 3837-3844.

[8] E.L. Rachofsky, E.Seibert, J.T. Stivers, R. Osman, J.B.A. Ross, *Biochemistry* **2001**, *40*, 957-967.

[9] D. Daujotyte, S. Serva, G. Vilkaitis, E. Merkiene, D. Venclovas, S. Klimasauskas, *Structure* **2004**, *12*, 1047-1055.

[10] G. Vilkaitis,A. Dong, E. Weinhold, X. Cheng, S. Klimasauskas, *J.Biol.Chem.* **2000**, *275*, 38722-38730.

[11] S.O. Kelley, J.K. Barton, *Science* **1999**, *283*, 375-381.

[12] M.A. O'Neill, H.C. Becker, C.Z. Wan, J.K. Barton,A.H. Zewail, *Angew Chem Int Ed* **2003**, *42*, 5896-5900.

[13] M.A. O'Neill, J.K. Barton, *J.Am.Chem.Soc.* **2002**, *124*, 13053-13066.

[14] M.A. O'Neill, J.K. Barton, *J.Am.Chem.Soc.* **2004**, *126*, 13234-13235.

[15] M.A. O'Neill, J.K. Barton, *J.Am.Chem.Soc.* **2004**, *126*, 11471-11483.

[16] M.A. O'Neill, J.K. Barton, *Proc.Natl.Acad.Sci.USA* **2002**, *99*, 16543-16550.

[17] C. Wan, T. Fiebig, S.O Kelley, C.R. Treadway, J.K. Barton, A.H. Zewail, *Proc.Natl.Acad.Sci.USA* **1999**, *96*, 6014-6019.

[18] R. Eritja,B.E. Kaplan, D. Mhaskar, L.C. Sowers, J. Petruska, M.F. Goodman, *Nucl.Acids.Res.* **1986**, *14*, 5869-5884.

[19] K. Evans, D.Xu, Y. Kim, T.M. Nordlund, *J.Fluoresc* **1992**, *2*, 209-216.

[20] E.L. Rachofsky, R. Osman, J.B.A. Ross, *Biochemistry* **2001**, *40*, 946-956.

[21] M. Kawai, M.J. Lee, K.O. Evans, T.M. Nordlund, *J.Fluoresc* **2001**, *11*, 23-32.

[22] R.K. Neely, S.W. Magennis,D.T.F. Dryden,A.C. Jones, *J.Phys.Chem.B* **2004**, *108*, 17606-17610.

[23] T.M. Nordlund, S. Andersson, L. Nilsson, R. Rigler, *Biochemistry* **1989**, *28*, 9095-9103.

[24] R.A. Hochstrasser, T.E. Carver, L.C. Sowers, D.P. Millar, *Biochemistry* **1994**, *33*, 11971-11979.

[25] C.R. G uest, R.A. Hochstrasser, L.C. Sowers, D.P. Millar, *Biochemistry* **1991**, *30*, 3271-3279.

[26] R.K. Neely, D. Daujotyte, S. Grazulis, S.W. Magennis, D.T.F. Dryden, S. Klimasauskas, A.C. Jones, *Nucleic Acids Res* **2005**, *33*, 6953-6960

[27] D.E. Lynch, I. McClenaghan, *Acta Crystallographica Section C-Crystal Structure Communications* **2003**, *59*, O53-O56.

[28] M.R. Harnden, R.L. Jarvest, A.M.Z. Slawin, D.J. Williams, *Nucleosdies Nucleotides* **1992**, *9*, 499.

[29] H.H. Chen, L.B. Clark, *J. Chem. Phys.* **1973**, *58*, 2593-2603.

[30] M. Rist, H.A. Wagenknecht,T. Fiebig, *ChemPhysChem* **2002**, *3*, 704-+.

[31] N.P. Johnson, W.A. Baase, P.H. von Hippel, *Proc.Natl.Acad.Sci.USA* **2004**, *101*, 3426-3431.

[32] R-X. He, X-H. Duan, X-Y. Li, *Phys.Chem.Chem.Phys.* **2006**, *8*, 587-591.

[33] A. Broo, A. Holmen, *Chem Phys* **1996**, *211*, 147-161.

[34] H.R. Drew, R.E. Dickerson,. *J.Mol Biol* **1981**, *151*, 535-556.

[35] M.A. El Hassan, C.R. Calladine, *Phil.Trans.Royal Soc.London, A* **1997**, *355*, 43-100.

[36] J.D. Wright, *Molecular Crystals*; Cambridge University Press: Cambridge, **1995**.

[37] D.P. Craig and S.H. Walmsley, *Éxcitons in Molceular Crystals: Theory and Applications*, W.A. Benjamin Inc., New York, **1968.**

[38] J.N. Murrell, J. Tanaka, *Mol. Phys.* **1964**, *7*, 363-380.

[39] A. Holmen, B. Norden, B. Albinsson, *J. Am. Chem. Soc.* **1997**, *119*, 3114-3121.

[40] J.M. Jean, K.B. Hall, *J. Phys. Chem. A* **2000**, *104*, 1930-1937.

[41] A.C. Borin, L.Serrano-Andres, V. Ludwig, K. Coutinho, S. Canuto, *Int. J. Quantum Chem.* **2006**, *106*, 2564-2577.

[42] K.A. Seefeld, C. Plutzer, D. Lowenich, T. Haber, R. Linder, K. Kleinermanns, J. Tatchen, C.M. Marian, *Phys. Chem. Chem. Phys.* **2005**, *7*, 3021-3026.

[43] M.A. O'Neill, C.Dohno, J.K. Barton, . *J .Am .Chem. Soc.* **2004**, *126*, 1316-1317.

[44] R.K. Neely, A.C. Jones, *J. Am. Chem. Soc*. **2006**, *128*, 15952-15953.

[45] O.J.G. Somsen, G. Trinkunas, M. Niels de Keijzer, A. Van Hoek, H. van Amerongen, *J. Luminescence* **2006**, *119-120*, 100-104.

[46] J.M. Jean, K.B. Hall, *Proc.Natl.Acad.Sci.USA* **2001**, *98*, 37-41.

[47] O.F.A. Larsen, I.H.M. van Stokkum, F.L. de Weerd, M. Vengris, C.T. Aravindakumar, R. van Grondelle, N.E. Geacintov, H. van Amerongen, *Phys.Chem.Chem.Phys.* **2004**, *6*, 154-160.

[48] G.M. Sheldrick, *SADABS, version 2004/1* 2004, University of Gottingen, Germany.

[49] A. Altomare, G. Cascarano, G. Giacovazzo, A. Guagliardi, M.C. Burla, G. Polidori, M. Camalli, *J.Appl.Cryst.* **2004**, *27*, 435.

[50] P.W. Betteridge, J.R. Carruthers, R.I. Cooper, K. Prout, D.J. Watkin, *J.Appl.Cryst.* **2003**, *36*, 1487.